Effect of the Slag Composition on the Process Behavior, Energy Consumption, and Nonmetallic Inclusions during Electroslag Remelting

Reinhold Schneider, Valentin Wiesinger, Siegfried Gelder, and Gerhard Reiter*

Electroslag remelting (ESR) is an important process to produce high-quality tool steels. The slag composition has a strong effect on the remelting behavior, particularly on energy consumption and the removal of nonmetallic inclusions (NMI). The latter aspect is strongly related to chemical reactions between the slag and the metal and determines the necessary composition of the slag. Also, the electrical conductivity of the slag is determined by the slag composition, and a high resistivity is desirable. The effect of different slag compositions with 0%–60% CaF_2 and a corresponding wide range of electrical conductivities is investigated regarding slag movement, slag surface temperature, and slag skin thickness, as well as their impact on chemical reactions and the removal of NMI. Therefore, a laboratory-scale ESR unit and the plastic mold steel X40Cr14 are used for the experimental trials. The results show a strong impact on the remelting behavior as well as on the specific energy consumption ranging from ≈900 to over 1700 kWh h^{-1}. The findings from the chemical analysis and detection of NMI indicate that a similar metallurgical behavior is feasible, leading to comparable amounts of dominantly Al_2O_3–MgO-type inclusions with some variation due to different activities in the slag.

1. Introduction

Electroslag remelting (ESR) is a well-established secondary refining process for many steels and Ni-base alloys with highest requirements regarding material properties. The main purposes are a dense solidification of ingots with a low degree of segregation as well as the reduction of medium-sized and especially complete removal of large nonmetallic inclusions (NMI). The specific energy consumption of ESR is documented in the range from 880 to over 2000 kWh t^{-1}.[1–7] Rising requirements regarding sustainability, emission control, and environmental protection have triggered new awareness for this topic.[4,8,9] Besides plant geometry and design, the customarily CaF_2-based slag plays the key role in the heat generation and energy consumption of ESR. Key properties are the melting point as well as the electrical and thermal conductivity.[2,10] Other factors such as fill ratio and the amount of slag, or the melt rate can also have a strong effect.[4,8,11–16]

According to Holzgruber,[16] rising fill ratios up to 0.4 lead to a reduction in specific energy consumption due to a better heat transfer into the electrode and less radiation losses at the free slag surface. A further increase in fill ratio surprisingly resulted in a reversed trend due to changing immersion depths. Results from Li et al.,[14] both laboratory scale and industrial size, demonstrate the strong effects of fill ratio (0.24 and 0.6) and electrical conductivity on the specific energy consumption with values below 1000 kWh t^{-1} at higher fill ratios combined with low or no CaF_2-containing slags. CaF_2-free slags in Brückmann and Schwerdtfeger[17] confirmed their particular advantage in specific energy consumption with values below 1000 kWh t^{-1}.

There are only few reports of systematic research on energy consumption in ESR on the industrial scale. A recent investigation with a wider variation of slags is documented in refs. [5-7], and confirms an almost linear increase with electrical conductivity. A similar but less pronounced increase is reported in Jäger and Kühnelt[18] for slag composition with a wide variety of CaF_2 contents and a significantly higher fill ratio. A recent summary on the different effects of the fill ratio and the electrical conductivity on the specific energy consumption can be found in Schneider et al.,[4] indicating that the energy consumption data from laboratory scale

R. Schneider
Research and Development
University of Applied Sciences Upper Austria
Stelzhamerstraße 23, 4600 Wels, Austria
E-mail: r.schneider@fh-wels.at

V. Wiesinger
University of Applied Sciences Upper Austria
Stelzhamerstraße 23, 4600 Wels, Austria

V. Wiesinger
K1-MET GmbH
Stahlstraße 14, Betriebsgebäude (BG) 88, 4020 Linz, Austria

S. Gelder, G. Reiter
voestalpine BÖHLER Edelstahl GmbH & Co KG
Mariazellerstraße 25, 8605 Kapfenberg, Austria

The ORCID identification number(s) for the author(s) of this article can be found under https://doi.org/10.1002/srin.202200483.

DOI: 10.1002/srin.202200483

experimental investigations can be transferred to industrial plants, when experiments are conducted with similar fill ratios.

Results of laboratory experiments using various amounts from 1.3 to 2.4 kg of a CaF_2-based slag are reported in El Gammal and von Hagen[13] and exhibit an almost 50% increase of the specific energy consumption with rising slag quantity. Such strong dependency on the slag cap height was also observed in Dewsnap and Schlatter[15] with an increase in energy consumption of 40% when rising the slag cap height from 75 to 125 mm. However, only a slight tendency of increasing energy consumption when raising the amount of slag from 3.5 to 6.5 kg was found in Schneider et al.,[4] indicating that other factors can contradict this effect. The effect of the melt rate in Schneider et al.[4] was found to be minor as well, lying between the results in refs. [11,13], which found almost no, and ref. [12] with a significant reduction on energy consumption with rising melt rate.

The practical use of low or no-CaF_2 slags is still restricted due to concerns regarding negative effects on the cleanliness levels as indicated in Duan and Guo.[9] A comparison after remelting using a slag of 40% CaF_2, 30% CaO, and 30% Al_2O_3 with CaF_2-free slags shows that, except for higher SiO_2 concentrations, good levels in cleanliness can also be achieved by all slags.[17] However, the investigated steel had a relatively high S content, hence improvements regarding cleanliness were dominantly connected with sulfur removal, which is not directly comparable with modern steelmaking praxis. Contrarily, according to Anable et al.,[19] CaF_2-free slags led to a limited cleaning effect compared to CaF_2-rich ones. Two more recent comparison using slags with different CaF_2 contents (32% and 14%) in Schneider et al.[4,20] showed no negative effect of a lower CaF_2 content in the number and dependency size of the NMI. Thereby it must be taken into consideration that cleanliness requirements have shifted from original sulfide removal toward oxide inclusion optimization.[20–24] The focus of this investigation was therefore to determine the effect of a wide variation of the CaF_2 content in the slag on process-related effects, especially energy consumption, as well as on quality-related aspects, primarily the content and type of NMI, using a state-of-the-art electrode material. Thereby the potential for significant energy savings without loss in product quality should be evaluated.

2. Experimental Section

2.1. Materials

The steel used for the remelting experiments was the corrosion-resistant plastic mood steel DIN EN X40Cr14 (AISI 420); its chemical composition can be found in **Table 1**. The electrodes had a diameter of 101.5 mm and a metallic bright surface.

Three slags chosen with varying amounts of CaF_2, ranging from 0% to nearly 60%, were used. The remainder consists of roughly equal amounts of CaO and Al_2O_3, with small additions of SiO_2 and MgO; their typical chemical compositions can be found in **Table 2**. All slags were standardized products of "Wacker Chemie AG" and were used in a premelted, granular form. Slags will be labeled regarding their approximate CaF_2 content, namely, $60CaF_2$, $30CaF_2$, and $0CaF_2$.

Table 1. Chemical composition of the electrode in [wt%].

C	Si	Mn	Cr	V	O	S
0.38	0.7	0.5	14.2	0.2	0.0003	0.0009

Table 2. Typical chemical compositions of the applied slags in [wt%] from ref. [25].

Commercial slag name	Abbreviation	CaF_2	CaO	Al_2O_3	SiO_2	MgO
ESR2022	$60CaF_2$	58.0	15.0	23.0	1.0	2.0
ESR2015	$30CaF_2$	31.5	29.5	33.5	1.5	3.0
ESR3002ELH	$0CaF_2$	0	47.0	46.0	$\leq$0.8	5.0

The electrical conductivity depending on the chemical composition and temperature can be calculated using the formulae from Hara et al.[26] The slag $60CaF_2$ has a high calculated electrical conductivity at 1600 °C of 2.53 Ω^{-1} cm^{-1}. The slag $30CaF_2$ is one of the standard slags in ESR with a medium electrical conductivity of 1.55 Ω^{-1} cm^{-1}, while the slag $0CaF_2$ is CaF_2-free and has the lowest electrical conductivity of 0.88 Ω^{-1} cm^{-1}.

2.2. Process Parameters

The experiments were performed on a laboratory scale ESR unit. The power supply operates at 4.5 Hz with a maximum voltage of 100 V and a maximum current of 5 kA. The used round mold was slightly conical with an average diameter of 168 mm. The voltage is mostly dependent on the immersion depth, the electrical conductivity, and amount of slag. The most important parameters are shown in **Table 3**. They were chosen to achieve a comparable melt rate of about 50 kg h^{-1} while ensuring a stable remelting behavior.

2.3. Process Data Recording and Slag Temperature Measurement

The electrical energy consumption and heat transfer, based on flow rate and the resulting temperature difference, to the cooling water were continuously measured throughout the remelting trials. Additional slag surface temperature measurements were performed with a two-color pyrometer (Keller PA41AF21/S) with an average spot size diameter of 5 ± 2 mm and were started when reaching a stable remelting behavior after 20 min.

2.4. Material Investigations

The ingots were forged, and samples were taken in the upper part of the ingot for chemical analysis and investigation of NMI, the

Table 3. Process parameters of the remelting experiments.

Slag	Slag amount [kg]	Current [kA]	Voltage [V]	Melt rate [kg h^{-1}]	Immersion [mm]
$60CaF_2$	5	4.7	60–62	47	15
$30CaF_2$	5	3.0	64–65	48	6
$0CaF_2$	5	2.7	60–62	53	3

latter was performed with an automated scanning electron microscopy with energy-dispersive X-ray spectroscopy (SEM-EDS) system. Details on the examination method can be found in Schneider et al.[20] NMI with an O content ≥5 wt% and an S:O ratio <0.15 were considered oxides. Inclusions with O and S contents ≥2 wt% each and an S:O ratio between 0.15 and 6.67 were categorized as oxysulfides (conglomerates/compounds of oxides and sulfides). NMI with an S content ≥2 wt% and an O:S ratio <0.15 were taken as sulfides.

3. Results

3.1. Specific Energy Consumption

The total specific energy consumption when remelting with the slag 60CaF_2 was 1736 kWh t^{-1}, for the slag 30CaF_2 it amounted to 1182 kWh t^{-1} while the slag 0CaF_2 had the lowest specific energy consumption with only 914 kWh t^{-1}. The distribution of the energy losses can be taken from **Figure 1**. The cooling of the base plate amounts to only 3%–4% of the energy dissipation during the stable remelting phase, while around 54%–59% of the energy are lost to the cooling of the mold. Independent of the slag used around 31%–34% of the energy consumption can be attributed to losses in the rectifier. The rest of the energy is lost to radiation of the slag surface and heat stored in the ingot, electrode, and plant components, which amounts to 5%–10%. It is clear that slags with a lower CaF_2 content, and therefore lower electrical conductivity, lead to a lower specific energy consumption.

3.2. Slag Surface Temperature and Slag Skin Thickness

To determine the true slag surface temperature, the temperature measurements from the two-color pyrometer were extrapolated to the mold height using a linear and power function, to account for radiation absorption due to smoke, and are displayed in **Figure 2**. Raising the CaF_2 content leads to an increased development of smoke, which due to absorption of radiation leads to a steeper incline and higher extrapolated slag surface temperature. **Figure 3** shows the slag skin thickness after remelting. While there is almost no change between 0 and about 30% CaF_2, the slag skin thickness is drastically lower for the high CaF_2-containing slag.

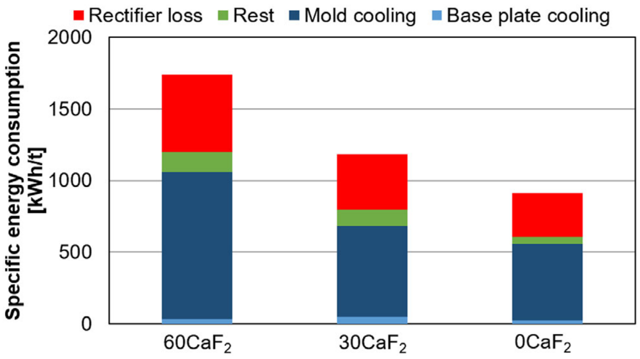

Figure 1. Specific energy consumption and distribution by cause of loss.

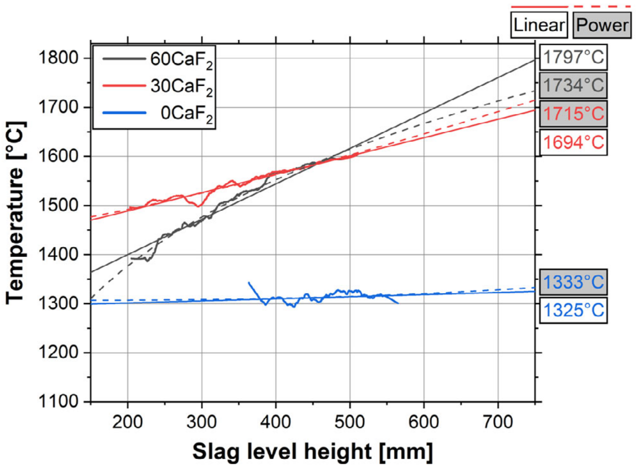

Figure 2. Smoothed slag surface temperature curves with linear and power extrapolations to the mold height.

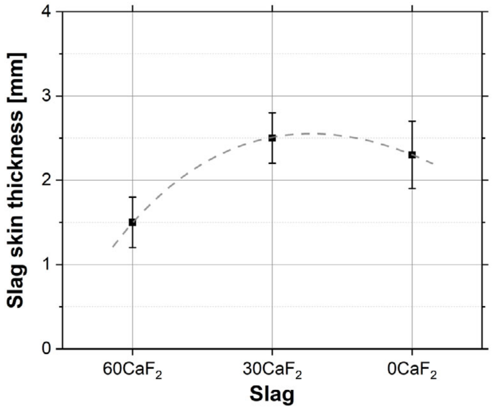

Figure 3. Slag skin thickness after remelting.

Higher viscosity slags with colder surfaces lead to lower heat losses due to radiation and energy transfer to the cooling water. The cellular appearance of the slag surface can be fine, as portrayed for slag 60CaF_2 in the left image in **Figure 4** or coarse as for slag 30CaF_2 in the center picture. High viscosity slags as seen in the right picture for slag 0CaF_2 have a darker and seemingly colder surface, broken up by surging slag that flows over the formed slag skin. A correlation between energy consumption and heat losses at the slag surfaces due to its behavior and appearance can be observed.

3.3. Effect of Slag Composition on NMI

Figure 5 gives an overview on the content and size distribution of NMI with an equivalent circle diameter (ECD) >3μm, comparing electrode and remelted ingots. A general decrease in the total amount in area percentage can be observed in all remelted ingots compared to the electrode, with the largest reduction for the CaF_2-free slag. As for NMI larger 6 μm (ECD), the most significant reduction was determined for the slag with 60% CaF_2. Differences can also be found in the type of NMI. The significant

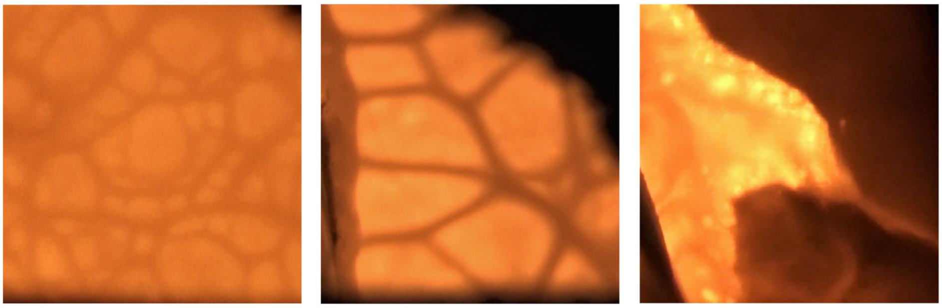

Figure 4. Surface of the slags $60CaF_2$, $30CaF_2$, and $0CaF_2$ (from left to right).

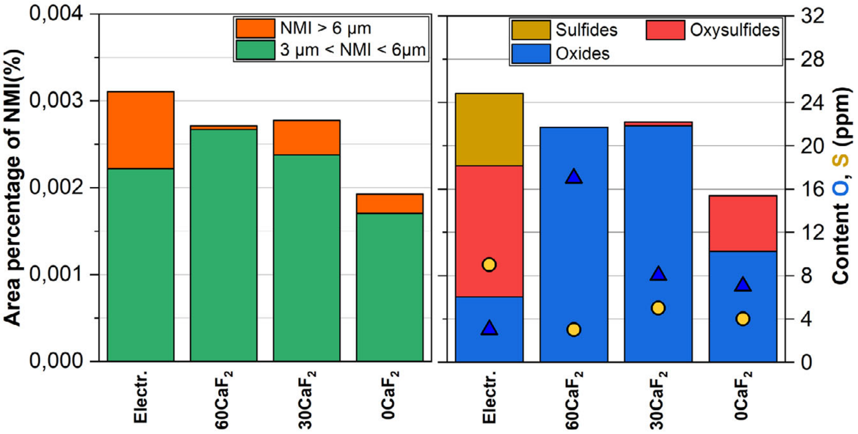

Figure 5. Amount in area percentage of NMI, classified by size and type, as well as O and S contents of the electrode and remelted ingots.

share of sulfides and oxysulfide conglomeratres in the electrode is strongly reduced during remelting. In reverse, increased O contents result in an increase of oxides. In case of slag $60CaF_2$, the strong increase in oxygen leads to many small oxides <3 µm ECD.

The composition of NMI is displayed in the ternary system Al_2O_3–SiO_2–MgO in **Figure 6**a–d, to which most of all detected oxides could be assigned. While white areas represent compositions without NMI, there is an increasing concentration from blue (few) to red (many NMI). Sulfides were always of MnS type and were not included in these figures.

Most of the NMI detected in the electrode were along the axis Al_2O_3–MgO, with a wider variation in composition and some CaO. After remelting, the desired MA-spinel-type inclusions (Al_2O_3.MgO) are predominantly formed after remelting with slags of lower CaF_2 composition and some Al_2O_3–(CaO) inclusions for slag $30CaF_2$. In contrast, remelting with the slag $60CaF_2$ leads to an NMI composition with a high Al_2O_3 content and some MgO.

4. Discussion

Direct surface temperature measurement is limited by the fume between the slag surface and the pyrometer, which according to refs. [10,27,28], is mainly caused through the evaporation of volatile fluorides such as CaF_2, AlF_3, and SiF_4. The extrapolated slag surface temperature increases dramatically when changing the flow behavior from lid formation and capping to a constantly liquid, cellular fluid flow pattern, but stays roughly constant at higher electrical conductivities despite observed small changes in the optical appearance of the slag surface. The observed high-temperature values of the higher CaF_2-containing slags correlate well with values in refs. [4,29–31]. On the contrary, both the flow behavior and the low slag surface temperature of the CaF_2 free slag are quite similar to results of a low CaF_2 slag in Schneider et al.[4] and correlate well with the trend found for CaF_2-free slags in Kusamichi et al.[30]

The slag skin thickness of slag $60CaF_2$ is around 40% lower than the other two slags. According to ref. [25], these slags have a similar melting point between 1350 and 1400 °C. Therefore, the lower slag skin thickness may be related to a higher flow velocity, which increases the heat transfer toward the mold wall.

A linear trend of the specific energy consumption with rising electrical conductivity can be observed in **Figure 7**. Data from refs. [5,14,21] support this linear trend, under consideration that, as described in Schneider et al.,[4] only experiments with a similar fill ratio, determined by the ratio of the cross-sectional area of electrode and mold, respectively (d^2/D^2), can be directly compared this way. In the case of the laboratory plant used, the fill ratio was 0.37. The comparatively high specific energy consumption of slag $60CaF_2$ might be additionally owed to the thinner slag skin and bigger loss of energy to the cooling water and to radiation but is still within the correlation range. In addition to the

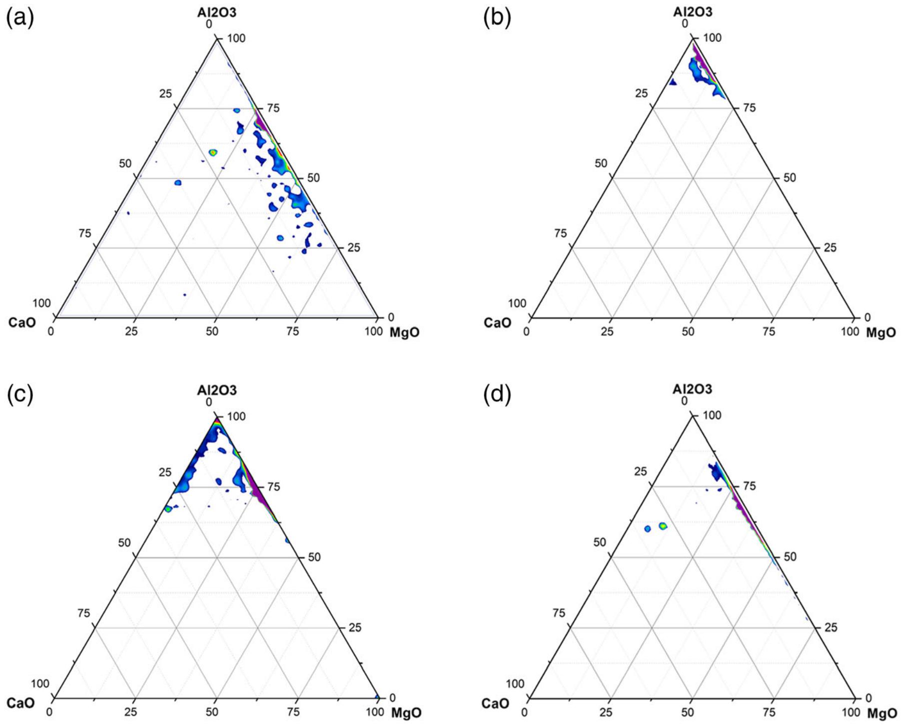

Figure 6. Chemical composition of the NMI in the ternary system CaO–MgO–Al_2O_3 a) in the electrode, and after remelting with the slags: b) $60CaF_2$, c) $30CaF_2$, and d) $0CaF_2$.

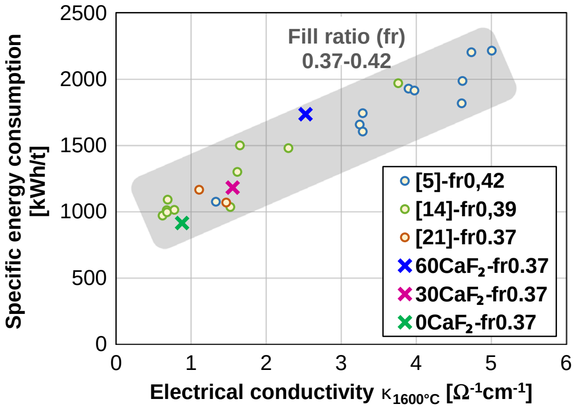

Figure 7. Specific energy consumption and its correlation with the electrical conductivity for remelting with a comparable fill ratio.

improved energy consumption, CaF_2-free slags reduce the environmental pollution caused by volatilization of fluorides and facilitate disposal according to refs. [9,32].

Changes in the NMI content, type, and composition after remelting are in good agreement with results in refs. [4,20,21,23,24] for slags with a medium to lower CaF_2 content. In refs. [22,33], the formation of predominantly alumina as well as Al_2O_3–CaO inclusions is reported using a similar steel and slag, but focusing on inclusions >8 μm, which might be surviving inclusions from the electrode and therefore not in equilibrium with the slag composition. As described in refs. [33,34], significant differences on the size distribution have to be expected. While in laboratory scale plants inclusion growth is rather limited, larger inclusion up to about 40 μm can be formed in large industrial ingots due to the growth of either newly formed or surviving inclusions from the electrode. Thereby it must be taken into consideration that NMI dissolution or absorption into the slag, as pointed out in refs. [34,35], are considered to be the two main mechanisms for the removal of NMI. Using low or no CaF_2-containing slags, which according to Milles and Keene[36] possess high viscosities, not only changes the flow behavior, but may therefore also affect the absorption process of NMI toward lower efficiency. Based on results in Li et al.,[37] a high CaO/Al_2O_3-ratio in the slag, corresponding to a lower viscosity, increases the dissolution of Al_2O_3 in CaF_2–CaO–Al_2O_3 slags, thereby indicating a way to improve the removal of alumina type inclusions. Remelting with the slag 70% $CaF_2 + 30\%Al_2O_3$, according to refs. [20,23,34], leads to mainly alumina type inclusion, which correlates well with the inclusions found for slag $60CaF_2$. The general effect of the Al_2O_3 content on the composition on the NMI composition is furthermore in good agreement with modeling results in Wang et al.[38] and experimental trials in refs. [39,40], making a balanced and well-adjusted Al_2O_3 contents a key factor for optimized slag compositions. The low amount of NMI after remelting with the CaF_2-free slag confirms the good results in Brückmann and Schwerdtfeger[17] for slags with a lower SiO_2 content. The activities of the slag components calculated by FactSage are shown in **Figure 8**.

The high Al_2O_3 activity and low MgO activity for the slag $60CaF_2$ support the formation of alumina type inclusions,

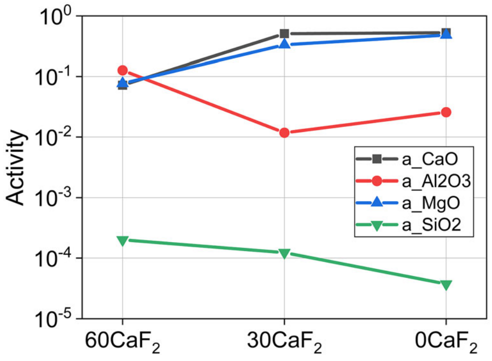

Figure 8. Activities of slag components for the slags used calculated with FactSage.

whereas the slags $0CaF_2$ and $30CaF_2$ have a significantly higher MgO activity and lower Al_2O_3 activity, which lead to the formation of Al_2O_3–MgO inclusions. Thereby the calculated activity values can describe the NMI formation much better than the measured Al_2O_3 activity data of the pure CaF_2–CaO–Al_2O_3 ternary system in Hino et al.[41] The importance of activity changes at constant Al_2O_3 content due to CaO additions is also documented in refs. [20,42], leading to higher MgO-containing NMI with rising CaO content in the slag. Generally, it must be taken into consideration that all remelting trials were conducted without protective gas, which according to refs. [20,23,43] increases the oxygen content.

The difference between the share of oxides and oxysulfides (conglomerates and compounds of oxides and sulfides) between the two lower CaF_2-containing slags despites similar O and S contents may be related to the defined criteria as inclusions. Below the threshold ration S:O-ratio <0.15, inclusion can still be oxysulfides but with a relatively small sulfide share. According to Mitchell and Sjöqvist Persson,[34] such conglomerates of compounds are typical for larger inclusions and named secondary inclusions in refs. [22,33].

5. Conclusion

Based on the results, the following main conclusion can be drawn: 1) An increase in CaF_2 content of the slag leads to more smoke formation, a higher slag surface temperature, and a lower slag skin thickness; 2) The corresponding increase of the electrical conductivity by raising the CaF_2 content results in a significantly higher specific energy consumption; 3) All slags used reduced the content of preferentially larger NMI, mainly the sulfides, combined with an increase of fine oxides due to open remelting in contact to air; 4) Based on changes in the activity of the slag components, the type of NMI after remelting changes from high-Al_2O_3-containing inclusions at high CaF_2 contents to MA-spinel-type inclusions for low and no CaF_2-containing slags; 5) The results indicate the potential to use slags with higher resistivity without significant losses in product quality; 6) More in-depth investigation, especially regarding the absorption of larger NMI, is necessary to clarify the cleaning effects of the different slags.

Acknowledgements

The authors gratefully acknowledge the funding support of K1-MET GmbH, metallurgical competence center. The research program of the K1-MET competence center is supported by COMET (Competence Center for Excellent Technologies), the Austrian program for competence centers. COMET is funded by the Federal Ministry for Climate Action, Environment, Energy, Mobility, Innovation and Technology, the Federal Ministry for Digital and Economic Affairs, the Federal States of Upper Austria, Tyrol and Styria as well as the Styrian Business Promotion Agency (SFG) and the Standortagentur Tyrol. Furthermore, Upper Austrian Research GmbH continuously supports K1-MET. Besides the public funding from COMET, this research project is partially financed by the scientific partner University of Applied Sciences—Upper Austria and the industrial partners voestalpine Böhler Edelstahl GmbH & Co KG and voestalpine Stahl Donawitz GmbH.

Conflict of Interest

The authors declare no conflict of interest.

Data Availability Statement

Research data are not shared.

Keywords

electroslag remelting, energy consumption, nonmetallic inclusions, slag compositions

Received: June 13, 2022
Revised: July 28, 2022
Published online:

[1] W. Holzgruber, E. Plöckinger, *Stahl Eisen* **1968**, *88*, 638.
[2] A. Mitchell, *J. Vac. Sci. Technol.* **1970**, *7*, 63.
[3] G. Hoyle, *Electroslag Process – Principles and Practice*, Applied Science Publishers, London, NY **1983**.
[4] R. Schneider, V. Wiesinger, S. Gelder, A. Mitchell, D. David, *ISIJ Int.* **2022**, *62*, 1199.
[5] J. Korp, Ph.D. Thesis, Montanuniversität Leoben, **2007**.
[6] J. Korp, R. Schneider, P. Presoly, W. Krieger, *Berg Hüttenmaenn. Monatsh.* **2008**, *153*, 175.
[7] P. Presoly, J. Korp, R. Schneider, *Arch. Metall. Mater.* **2008**, *53*, 1.
[8] Y.-L. Xiong, Z.-W. Song, A.-G. Wang, Y.-C. Lou, *China Foundry*, **2019**, *16*, 1.
[9] S.-D. Duan, H.-J. Guo, *Steel Res. Int.*, **2020**, *91*, 1900634.
[10] A. Mitchell, *Proc. 2005 Int. Symp. on Liquid Metal Processing and Casting (LMPC 2005)*, ASM Inter., Santa Fe, September 2005.
[11] S. F. Medina, M. P. de Andrés, *Rev. Metal. CENIM* **1983**, *19*, 271.
[12] T. El Gammal, F. A. Denkhaus, *Stahl Eisen* **1989**, *109*, 1171.
[13] T. El Gammal, I. von Hagen, Grundlagen der Raffination eines einfachen Baustahles nach dem Elektro-Schlacke-Umschmelzverfahren, Forschungsbericht des Landes Nordrhein-Westphalen Nr., Westdeutscher Verlag, Opladen, Germany **1976**.
[14] Z. Li, J. Zhang, J. Jiang, W. Cui, *Proc. 7th Int. Conf. Vacuum Metallurgy: special meltings and metallurgical coatings - ICVM*, Japan Institute of Metals, Tokyo, November 1982, p. 1486.
[15] P. Dewsnap, R. Schlatter, *Proc. 5th Int. Symp. on Electroslag and other Special Melting Technologies*, Pittsburgh, October 1974, p. 91.
[16] W. Holzgruber, *Radex-Rundsch.* **1975**, 409.

[17] G. Brückmann, K. Schwerdtfeger, *Stahl Eisen* **1983**, *103*, 387.

[18] H. Jäger, G. Kühnelt, *Berg Hüttenmaenn. Monatsh.* **1975**, *125*, 423.

[19] W. E. Anable, R. H. Nafzinger, D. C. Robinson, *J. Met.* **1973**, *2*, 55.

[20] R. Schneider, M. Molnar, S. Gelder, R. Reiter, C. Martinez, *Steel Res. Int.* **2018**, *89*, 1800161.

[21] R. Schneider, C. Schüller, P. Würzinger, G. Reiter, C. Martinez, *Berg Hüttenmaenn. Monatsh.* **2015**, *160*, 117.

[22] E. Sjöqvist Persson, A. Karasev, A. Mitchell, P. G. Jönsson, *Metals*, **2020**, *10*, 1620.

[23] Y.-W. Dong, Z.-H. Jiang, Y.-L. Cao, A. Yu, D. Hou, *Metall. Mater. Trans. B* **2014**, *45B*, 1315.

[24] H. Wang, C.-M. Shi, J. Li, C.-B. Shi, Y.-F. Qi, *Ironmaking Steelmaking*, **2018**, *45*, 6.

[25] Wacker Chemie AG, Produktkatalog Electroflux **2021**.

[26] S. Hara, H. Hashimoto, K. Ogino, *Trans. Iron Steel Inst. Jpn.* **1983**, *23*, 1053.

[27] A. Mitchell, R. M. Smailer, *Int. Met. Rev.* **1979**, *24*, 231.

[28] J.-T. Ju, G.-H. Ji, C.-M. Tang, J.-L. An, *Steel Res. Int.* **2020**, *91*, 2000111.

[29] A. Mitchell, S. Joshi, *Metall. Trans.* **1973**, *4*, 631.

[30] T. Kusamichi, T. Ishii, T. Onoye, K. Narita, *Tetsu to Hagane* **1980**, *66*, 48.

[31] Y. Oguti, Y. Tanbe, S. Miyama, A. Ejima, *Tetsu to Hagane* **1977**, *63*, 210.

[32] D. Zheng, J. Li, C. Shi, *ISIJ Int.* **2020**, *60*, 5.

[33] E. Sjöqvist Persson, S. Brorson, A. Mitchell, P. G. Jönsson, *Metals*, **2021**, *11*, 408.

[34] A. Mitchell, E. Sjöqvist Persson, *Ironmaking Steelmaking* **2022**, *49*, 1.

[35] C.-B. Shi, S.-J. Wang, J. Li, J.-W. Cho, *J. Iron Steel Res. Int.* **2021**, *28*, 1483.

[36] C. K. Milles, B. J. Keene, *Int. Met. Rev.* **1981**, *1*, 21.

[37] J. L. Li, Q. F. Shu, Y. A. Liu, K. C. Chou, *Ironmaking Steelmaking*, **2014**, *41*, 732.

[38] J. Wang, L. Zhang, T. Wen, Y. Ren, W. Yang, *Metall. Mater. Trans. B* **2021**, *52B*, 1521.

[39] R. S. E. Schneider, M. Molnar, G. Klösch, C. Schüller, *Metall. Mater. Trans. B* **2020**, *51B*, 1904.

[40] R. S. E. Schneider, M. Molnar, G. Klösch, C. Schüller, J. Fasching, *Steel Res. Int.*, **2020**, *91*, 2000241.

[41] M. Hino, S. Kinoshita, H. Ito, S. Yorozuya, *CAMP-ISIJ* **1994**, *7*, 41.

[42] D. Huo, D.-Y. Wang, Z. H. Jiang, T.-P. Qu, H.-H. Wang, J.-W. Dong, *Metall. Mater. Trans. B* **2021**, *52B*, 478.

[43] C.-B. Shi, X.-C. Chen, H.-J. Guo, Z.-J. Zhu, H. Ren, *Steel Res. Int.* **2012**, *83*, 472.